Trans. Phenom. Nano Micro Scales, 8(1): 1-8, Winter and Spring 2020
DOI: 10.22111/tpnms.2019.30672.1180

ORIGINAL RESEARCH PAPER

Analytical Approach for Vibration Analysis of a Microsensor with Two layers of Silicon and Piezoelectric based on MCST

Abbas Rahi*

Faculty of Mechanical and Energy Engineering, Shahid Beheshti University, Tehran, Iran

Received 26 June 2019; revised 13 July 2019; accepted 1 October 2019; available online 22 February 2020

ABSTRACT: The vibration analysis is an important step in the design and optimization of microsensors. In most of the cases, COMSOL software is employed to consider the size-dependency on the dynamic behavior in the MEMS sensors. In this paper, the Modified Couple Stress Theory (MCST) is used to capture the size effect on dynamic behavior in a microsensor with two layers of the silicon and piezoelectric. The governing equations of the system and also associated boundary conditions are derived based on the MCST and using Hamilton's principle by obtaining the total kinetic and potential energies of the system. Then, the obtained governing equations are solved using an analytical approach to determine the natural frequencies of the system. The first, second and third natural frequencies of the microsensor are determined using an analytical approach. Finally, the natural frequency variations of the system are presented with respect to different values of the system parameters such as dimensionless parameters of the sensor geometric, the thickness of the silicon and piezoelectric layers and also the dimensionless material length scale parameter. The obtained results show that the material length scale parameter values and also the length, width, and thickness of each layer of the sensor are extremely effective on the vibration characteristics of the piezoelectric cantilever-based Micro Electro Mechanical System (MEMS) sensors. Also, the results show that the first natural frequency of the microsensor will decrease with either increasing dimensionless material length scale parameter or decreasing the thickness of silicon and piezoelectric. This analytical approach presents an efficient method to predict the dynamic behavior of microsensors and consequent optimization in their design procedure.

KEYWORDS: *Free vibration; MEMS; Microsensor; Modified couple stress theory; Piezoelectric; Size-dependency*

INTRODUCTION

Dynamic behavior study of Micro-Electro-Mechanical-System (MEMS) devices is very important to the design and optimization of a small component of the equipment. Nowadays, manufacturing of small size devices in the field of the MEMS is possible with the development of new technologies. Microbeams are one of the most common elements which are used in the field of the MEMS sensors [1-8].

Several of the researchers studied the dynamic behavior of the micro-components in the field of MEMS based on the classical continuum mechanics theories or using the Finite Element Method (FEM) [9-11].

In recent years, it has been observed that the classical continuum mechanics theories are unable to predict and explain the static and dynamic behaviors of the materials in small sizes such as microbeams [12-16]. In other words, capture and consideration of the size effect are a significant challenge in the study of the dynamic behaviors of the small size structures. Therefore, several of the non-classical continuum theories such as nonlocal elasticity theory, strain gradient theory, and couple stress theory, have been presented to capture the size effect in dynamic response for micro components [17-22].

*Corresponding Author Email: *a_rahi@sbu.ac.ir*
Tel.: +982173932686; Note. This manuscript was submitted on June 26, 2019; approved on October 01, 2019; published online February 22, 2020.

Mindlin and Eshel [18] proposed a higher-order continuum theory to consider the size effect by using the first and second gradients of the strain tensor. Then, Fleck and Hutchinson [19] reformulated Mindlin's theory also known as the Strain Gradient Theory (SGT). Afterward, Lam et al. [20] presented the Modified Strain Gradient Theory (MSGT) to consider the size dependency of the materials mechanical behavior by the use of three constants of material length scale parameters. The couple stress theory was also introduced by Mindlin and Tiersten [21] as a non-classical continuum theory to consider the size dependency effect in microsystems using two material length scale parameters. Then, Yang et al. [22] suggested the Modified Couple Stress Theory (MCST) which uses one material length scale parameter to capture the size effect in micro components. It should be noted that the MCST is a special case of the Modified Strain Gradient Theory (MSGT) where the two first constants of material length scale parameters are set to zero. The MCST has been used by several researchers to investigate the size effect in the static and dynamic behaviors of materials in micro components. For example, the MCST has been employed as a basic formulation to capture the size dependency in static or dynamic behavior of microbeams [23-30], and mechanical behaviors of microplates [31-37], and vibration response of rotating microbeams [38].

Nomenclature

A	cross section area (m^2)	$\theta_{i,j}$	gradient of rotation
E	Young's modulus	λ, μ	Lamé constants
h	Thickness (μm)	ϑ	Poisson's ratio
$\bar{I}_{yy}$	cross-section area-moment of inertia	π_s	strain energy
L	length (μm)	ρ	density (kg/m^3)
l	material length scale parameter	σ_{ij}	stress tensor
m_{ij}	deviatoric part of the symmetric couple stress tensor	ω	natural frequency (rad/s)
u_i	components of the displacement vector	χ^s_{ij}	symmetric curvature tensor
T	kinetic energy of the system	δW	virtual work
t	Time (s)		**Subscripts**
w	width (μm)	FEM	Finite Element Method
$w(x,t)$	transverse deflection	MCST	Modified Couple Stress Theory
	Greek Symbols	MEMS	Micro-Electro-Mechanical-System
ε_{ij}	strain tensor	MSGT	Modified Strain Gradient Theory
ϵ_{ijk}	alternating tensor or permutation symbol	SGT	Strain Gradient Theory
θ_i	infinitesimal rotation vector		

Also, Li and Luo [39] investigated the flexoelectric effect of piezoelectric microbeam based on the MCST. Shoaib et al. [40-41] studied the vibration and frequency analysis of electrostatic cantilever-based MEMS sensors. They investigated the frequency, displacement and functional parameters of the sensors without any fault. Also, the effect of crack faults on the dynamic response of a piezoelectric cantilever-based MEMS sensor was studied by Shoaib et al. [42] using the COMSOL software. In the present article, the vibration analysis of a microsensor with two layers of silicon and piezoelectric (PZT: Lead Zirconate Titanate) is studied using an analytical approach based on the MCST. The microsensor is modeled by a cantilever beam with two layers of silicon and PZT that are interconnected. The governing equations of lateral vibration and the associated boundary conditions are obtained based on the MCST and using Hamilton's principle. Then, the obtained governing equations are solved using an analytical approach to determine the natural frequencies of the system. Finally, the first, second and third natural frequencies of the microsensor are investigated with respect to the different values of the system parameters such as the thickness of the silicon and piezoelectric layers, dimensionless material length scale parameter and dimensionless parameters of the length and width of the sensor. The obtained results show that the material length scale parameter values and also the length, width, and thickness of each layer have significant effects on the natural frequencies of the system.

DEFINITION AND MODELING OF THE SYSTEM

The modeling and the geometry of a microsensor with two layers of the silicon and piezoelectric are shown in Figure 1. The microsensor consisted of a cantilever beam containing Silicon and Piezoelectric layers with the width w, length L, and total thickness h. The silicon layer (layer No. 1) has length L, width w, thickness h_1, density ρ_1, Young's modulus E_1, and Poisson's ratio ϑ_1. Also, the piezoelectric layer (layer No. 2) has length L, width w, thickness h_2, density ρ_2, Young's modulus E_2, and Poisson's ratio ϑ_2 . In addition, the coordinate system X-Y-Z, middle surface, and neutral surface have been shown in Figure 1. It should be noted that for multi-layer microplates with different materials and different elasticity modulus, the middle surface (mid-plane) and the neutral surface of the cantilever beam are not coincident. The z_m and z_n are the transverse coordinates defined with respect to the middle surface and neutral surface of the cantilever microplate, respectively (please see Fig. 1).

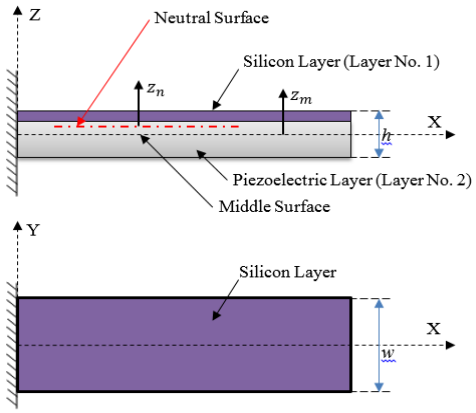

Fig. 1. Modelling of the microsensor with two layers

For functionally graded materials, the position of the neutral surface with respect to the middle surface can be determined as [32]:

$$e = \frac{\int_{\frac{-h}{2}}^{\frac{+h}{2}} (E)(z_m)\, dz_m}{\int_{\frac{-h}{2}}^{\frac{+h}{2}} E\, dz_m} \tag{1}$$

where Young's modulus E is considered to vary continuously in the thickness direction.

For a micro beam with two layers, equation 1 can be simplified to obtain the following equation for determination of the neutral surface position with respect to the middle surface.

$$e = \frac{1}{2}\ \frac{(E_2 - E_1)(h_2^2 - h\ h_2)}{E_1\ h + (E_2 - E_1)h_2} \tag{2}$$

MODELING AND GOVERNING EQUATIONS OF THE SYSTEM

The strain energy of a linear elastic isotropic material based on the modified couple stress theory can be written as follows [24, 32]:

$$\pi_s = \frac{1}{2}\ \int_V \left(\ \sigma_{ij}\varepsilon_{ij} + m_{ij}\ \chi_{ij}^s\right) dV\ ;\ i = x, y, z \tag{3}$$

where V denotes the volume of the system. In addition, the components of the stress tensor σ_{ij}, the strain tensor ε_{ij}, the deviatoric part of the symmetric couple stress tensor m_{ij} and the symmetric curvature tensor χ_{ij}^s can be expressed as follows:

$$\sigma_{ij} = 2\mu\varepsilon_{ij} + \lambda\varepsilon_{kk}\delta_{ij} \quad ; \quad m_{ij} = 2\mu l^2\chi_{ij}^s \tag{4}$$

$$\varepsilon_{ij} = \frac{1}{2}\left(u_{i,j} + u_{j,i}\right) \quad ; \quad \chi_{ij}^s = \frac{1}{2}\left(\theta_{i,j} + \theta_{j,i}\right) \tag{5}$$

$$\theta_i = \frac{1}{2}\epsilon_{ijk}\ u_{k,j} \tag{6}$$

In the above equations, $\theta_{i,j}$ is the gradient of rotation, θ_i is infinitesimal rotation vector, ϵ_{ijk} is alternating tensor (or permutation symbol), and u_i is components of the displacement vector.

The parameters (λ, μ) and l are called Lamé constants and the material length scale parameter, respectively. The Lamé constants can also be written regarding Young's modulus E and Poisson's ratio ϑ as follows:

$$\lambda = \frac{\vartheta\ E}{(1+\vartheta)(1-2\vartheta)} \quad ; \quad \mu = \frac{E}{2(1+\vartheta)} \tag{7}$$

Consider that the $w(x,t)$ denotes the transverse deflection of the neutral line of the microsensor with two layers at any point x along the length of the sensor in the Z direction (please see Fig. 1).

By using Euler-Bernoulli beam theory, the displacement field at any material point in the microbeam can be written as follows [32]:

$$u_1 = z_n\frac{\partial w(x,t)}{\partial x} \quad ; \quad u_2 = 0 \ ; \ u_3 = w(x,t) \tag{8}$$

Assuming small transverse deflection in the microsensor, the non-zero components of the strain and the stress tensors can be expressed as follows:

$$\varepsilon_{xx} = z_n\frac{\partial^2 w}{\partial x^2}$$
$$\sigma_{xx} = E\varepsilon_{xx} = \begin{cases} E_1 z_n\dfrac{\partial^2 w}{\partial x^2} & \text{(for layer No. 1)} \\ E_2 z_n\dfrac{\partial^2 w}{\partial x^2} & \text{(for layer No. 2)} \end{cases} \tag{9}$$

The non-zero components of the symmetric curvature tensor and the deviatoric part of the symmetric couple stress tensor can be obtained as follows:

$$\chi_{xy}^s = \chi_{yx}^s = \frac{-1}{2}\frac{\partial^2 w}{\partial x^2}$$
$$m_{xy} = m_{yx}$$
$$= \begin{cases} -\dfrac{E_1\ l_1^2}{2(1+\vartheta_1)}\dfrac{\partial^2 w}{\partial x^2} & \text{(for layer No. 1)} \\ -\dfrac{E_2\ l_2^2}{2(1+\vartheta_2)}\dfrac{\partial^2 w}{\partial x^2} & \text{(for layer No. 2)} \end{cases} \tag{10}$$

where l_1 and l_2 are the material length scale parameters of the layers No. 1 and No. 2, respectively.

Therefore, from equation 3, the total strain energy of the system can be written as follows:

$$\pi_s = \frac{1}{2}\int_L\left[\int_A\left(\ \sigma_{ij}\varepsilon_{ij} + m_{ij}\ \chi_{ij}^s\right) dA\right] dx$$
$$= \frac{1}{2}\int_L\left[\int_A\left(\ \sigma_{xx}\varepsilon_{xx} + 2\ m_{xy}\ \chi_{xy}^s\right) dA\right] dx$$
$$= \frac{1}{2}\int_0^L\left[\left(E_1\ \tilde{I}_{yy1} + E_2\ \tilde{I}_{yy2}\right)\left(\frac{\partial^2 w}{\partial x^2}\right)^2\right] dx$$
$$+\ \frac{1}{2}\int_0^L\left[\left(\frac{E_1\ l_1^2}{2(1+\vartheta_1)}A_1\right.\right.$$
$$\left.\left.+\frac{E_2\ l_2^2}{2(1+\vartheta_2)}A_2\right)\left(\frac{\partial^2 w}{\partial x^2}\right)^2\right] dx \tag{11}$$

Where

$$\tilde{I}_{yy1} = \bar{I}_{yy1} + A_1\ \bar{z}_{n1}^2\ ,\ \tilde{I}_{yy2} = \bar{I}_{yy2} + A_2\ \bar{z}_{n2}^2$$
$$\bar{I}_{yy1} = \frac{w\ h_1^3}{12}\ ,\bar{I}_{yy2} = \frac{w\ h_2^3}{12}$$
$$A_1 = wh_1\ ,\ \ A_2 = wh_2$$
$$\bar{z}_{n1} = \frac{1}{2}(h - h_1 - 2e)$$
$$\bar{z}_{n2} = \frac{-1}{2}(h - h_2 + 2e) \tag{12}$$

Where A_1 and A_2 are the cross section areas of the layers No. 1 and No.2 at position x in length of the sensor.

It is noted that for a uniform and isotropic elastic with rectangular section ($w \times h_i$), the cross-section area-moment of inertia can be calculated from $\bar{I}_{yyi} = \frac{w h_i^3}{12} = \frac{A_i\, h_i^2}{12}$ for $i = 1, 2$.

Therefore, according to equation 11, the total strain energy of the system can be written as follows:

$$\pi_s = \frac{1}{2}\left\{\left(E_1\,\tilde{I}_{yy1} + E_2\,\tilde{I}_{yy2}\right) + \left[\frac{6\,E_1\,\bar{I}_{yy1}}{(1+\vartheta_1)}\left(\frac{l_1}{h_1}\right)^2 + \frac{6\,E_2\,\bar{I}_{yy2}}{(1+\vartheta_2)}\left(\frac{l_2}{h_2}\right)^2\right]\right\}\left[\int_0^L \left(\frac{\partial^2 w}{\partial x^2}\right)^2 dx\right] \tag{13}$$

The kinetic energy of the system T can be written as follows:

$$T = \frac{1}{2}\int_0^L \left[(\rho_1 A_1 + \rho_2 A_2)\,\dot{w}^2 + \left(\rho_1\,\tilde{I}_{yy1} + \rho_2\,\tilde{I}_{yy2}\right)\left(\frac{\partial \dot{w}}{\partial x}\right)^2\right] dx \tag{14}$$

where the dot over variables is the derivative of variable relative to time.

Hamilton's principle is considered as follows:

$$\int_{t_1}^{t_2} \delta(T - \pi_s + W)\, dt = 0 \tag{15}$$

where δW is the virtual work done by external non-conservative forces on the system. For free vibration analysis of the considered system, the δW is zero.

By substituting the equation 13 and 14 into 15, and then using variational calculus, governing equations of motion of the system can be derived as follows:

$$S\frac{\partial^4 w}{\partial x^4} + B\,\ddot{w} - D\frac{\partial^2 \ddot{w}}{\partial x^2} = 0 \tag{16}$$

where

$$S = \left(E_1\,\tilde{I}_{yy1} + E_2\,\tilde{I}_{yy2}\right) + \left[\frac{6\,E_1\,\bar{I}_{yy1}}{(1+\vartheta_1)}\left(\frac{l_1}{h_1}\right)^2 + \frac{6\,E_2\,\bar{I}_{yy2}}{(1+\vartheta_2)}\left(\frac{l_2}{h_2}\right)^2\right]$$
$$B = (\rho_1 A_1 + \rho_2 A_2)$$
$$D = \left(\rho_1\,\tilde{I}_{yy1} + \rho_2\,\tilde{I}_{yy2}\right) \tag{17}$$

By neglecting $\frac{\partial^2 \ddot{w}}{\partial x^2}$, the equation 16 can be simplified as follows:

$$S\frac{\partial^4 w}{\partial x^4} + B\,\ddot{w} = 0 \tag{18}$$

The solution of equation 18 can be expressed as follows:

$$w(x,t) = W(x) \times \sin(\omega t) \tag{19}$$

By substituting equation 19 into equation 18 and to have some algebraic simplification, we have

$$\frac{d^4 W}{dx^4} - \beta^4 W(x) = 0\,,\ \beta^4 = \frac{B\,\omega^2}{S} \tag{20}$$

where ω is the natural frequency.

Also, the general solution of equation 20 can be obtained as follows:

$$W(x) = \tilde{B}_1 \sin(\beta x) + \tilde{B}_2 \cos(\beta x) + \tilde{B}_3 \sinh(\beta x) + \tilde{B}_4 \cosh(\beta x) \tag{21}$$

where $\tilde{B}_1$, $\tilde{B}_2$, $\tilde{B}_3$, and $\tilde{B}_4$ are constants.

The boundary conditions of the system can be expressed as follows:

$$W(0) = 0 \quad ; \quad \frac{dW}{dx}(0) = 0$$
$$\frac{d^2 W}{dx^2}(L) = 0 \quad ; \quad \frac{d^3 W}{dx^3}(L) = 0 \tag{22}$$

By substituting equation 22 into equation 21, a set of four algebraic equations resulting in matrix form can be obtained as follows:

$$\left[Q_{ij}\right]\left\{\tilde{B}_j\right\} = 0 \quad ; \quad i,j = 1,2,3,4 \tag{23}$$

where

$$Q_{11} = Q_{13} = 0\ ;\ Q_{12} = Q_{14} = 1$$
$$Q_{22} = Q_{24} = 0\ ;\ Q_{21} = Q_{23} = -\beta$$
$$Q_{31} = -\beta^2\, sin(\beta L)\ ;\ Q_{32} = -\beta^2\, cos(\beta L)$$
$$Q_{33} = \beta^2\, sinh(\beta L)\ ;\ Q_{34} = \beta^2\, cosh(\beta L)$$
$$Q_{41} = -\beta^3\, cos(\beta L)\ ;\ Q_{42} = \beta^3\, sin(\beta L)$$
$$Q_{43} = \beta^3\, cosh(\beta L)\ ;\ Q_{44} = \beta^3\, sinh(\beta L) \tag{24}$$

For nontrivial solution of equation 23, the determinant of the matrix $\left[Q_{ij}\right]$ must be zero. Also, if the determinant of the matrix $\left[Q_{ij}\right]$ is zero, the result and the first, second, third and fourth roots of it can be calculated as follows:

$$\det\left[Q_{ij}\right] = 0$$
$$\Rightarrow cos(\beta_n L)\, cosh(\beta_n L) = -1\ ;\ n = 1, \dots, \infty$$
$$\beta_1 L = 1.87510\ \ ;\ \ \beta_2 L = 4.69409\ \ ;$$
$$\beta_3 L = 7.85476\ \ ;\ \ \beta_4 L = 10.99554 \tag{25}$$

Therefore, according to equation 20 and 17, the natural frequencies of the microsensor with two layers can be determined as follows:

$$\omega_n = (\beta_n L)^2 \left[\frac{S}{B\,L^4}\right]^{\frac{1}{2}} = (\beta_n L)^2 \left[\frac{N_1 + N_2}{(\rho_1 h_1 + \rho_2 h_2) w L^4}\right]^{\frac{1}{2}} \tag{26}$$

where

$$N_1 = E_1 w h_1 \left(\frac{h_1^2}{12} + \bar{z}_{n1}^2\right) + E_2 w h_2 \left(\frac{h_2^2}{12} + \bar{z}_{n2}^2\right)$$
$$N_2 = \frac{E_1 w h_1^3}{2(1+\vartheta_1)}\left(\frac{l_1}{h_1}\right)^2 + \frac{E_2 w h_2^3}{2(1+\vartheta_2)}\left(\frac{l_2}{h_2}\right)^2 \quad (27)$$
$$\bar{z}_{n1} = \frac{1}{2}\left(h - h_1 - \frac{e}{2}\right)$$
$$\bar{z}_{n2} = \frac{1}{2}\left(h - h_2 - \frac{e+h_1}{2}\right)$$

VERIFICATION

In the previous section, the governing equation equation 18 for lateral vibration of the cantilever microbeam with two interconnected layers was derived analytically based on the MCST as follows:

$$\left\{\left(E_1 \tilde{I}_{yy1} + E_2 \tilde{I}_{yy2}\right) + \left[\frac{6\,E_1\,\bar{I}_{yy1}}{(1+\vartheta_1)}\left(\frac{l_1}{h_1}\right)^2 + \frac{6\,E_2\,\bar{I}_{yy2}}{(1+\vartheta_2)}\left(\frac{l_2}{h_2}\right)^2\right]\right\}\frac{\partial^4 w}{\partial x^4} + (\rho_1 A_1 + \rho_2 A_2)\ddot{w} = 0 \quad (28)$$

where

$$\tilde{I}_{yy1} = \bar{I}_{yy1} + A_1\,\bar{z}_{n1}^2\,;\ \tilde{I}_{yy2} = \bar{I}_{yy2} + A_2\,\bar{z}_{n2}^2$$
$$\bar{I}_{yy1} = \frac{w\,h_1^3}{12} \quad ; \quad \bar{I}_{yy2} = \frac{w\,h_2^3}{12}$$
$$A_1 = w h_1 \quad ; \quad A_2 = w h_2 \quad (29)$$
$$\bar{z}_{n1} = \frac{1}{2}(h - h_1 - 2e)$$
$$\bar{z}_{n2} = \frac{-1}{2}(h - h_2 + 2e)$$

In special case $\frac{l_i}{h_i} \approx 0$, for the macro system, the equation 28 is simplified as

$$\left(E_1 \tilde{I}_{yy1} + E_2 \tilde{I}_{yy2}\right)\frac{\partial^4 w}{\partial x^4} + (\rho_1 A_1 + \rho_2 A_2)\,\ddot{w} = 0 \quad (30)$$

Also, It can be easily seen that for the special case $h_2 = 0$ or $h_1 = 0$ (when we have only one layer), the equation 30 is simplified as

$$\left(E_1 \bar{I}_{yy1}\right)\frac{\partial^4 w}{\partial x^4} + (\rho_1 A_1)\,\ddot{w} = 0 \quad \text{or}$$
$$\left(E_2 \bar{I}_{yy2}\right)\frac{\partial^4 w}{\partial x^4} + (\rho_2 A_2)\,\ddot{w} = 0 \quad (31)$$

The equation 31 is compatible with the classical form of the governing equations of free vibration of a cantilever beam in macro size.

In addition, it is worth mentioning that according to Figure 2, in special case $h_2 = h_2 = 20\mu m$, the first natural frequency of the microsensor has been calculated to be 45 kHz based on the MCST using the data of Table 1. Also, according to Ref. [42], the first natural frequency of the microsensor has been reported to be 45.43 kHz using from the COMSOL software. Therefore, the above two approaches are in good agreement with each other.

RESULTS AND DISCUSION

In this section, the effect of size and also dimensions of the microsensor with two layers of silicon and piezoelectric on the natural frequencies of the system are investigated. In numerical analyses, according to Figure 1, the nominal dimensions, materials, and geometry of the microsensor are mentioned in Table 1 [42]. In the present paper, the material length scale parameters l_1 and l_2 for silicon and piezoelectric layers have been considered 1.0μm and 2.4μm, respectively. It should be noted that the mentioned values of the material length scale parameters have been estimated according to COMSOL results which are presented in [42].

Table1
Dimensions and material parameters of the microsensor [42].

Parameters description	**Symbol**	**unit**	**Layer No. 1 (Silicon layer) $i = 1$**	**Layer No. 2 (Piezoelectric layer) $i = 2$**
Length	L	μm	800	800
Width	w	μm	300	300
Thickness	h_i	μm	20	20
Young's modulus	E_i	GPa	170	63
Density	ρ_i	Kg/m^3	2233	7550
Poisson's ratio	ϑ_i	---	0.22	0.32

The first natural frequency of the microsensor versus the ratio thickness of the piezoelectric layer to thickness of the silicon layer ($\frac{h_2}{h_1}$) has been presented in Figure 2, for different values of the silicon thickness h_1.

Obtained results in Figure 2 show that the first natural frequencies of the system will increase with an increase in silicon layer thickness and increase of the dimensionless thickness of layers $\frac{h_2}{h_1}$.

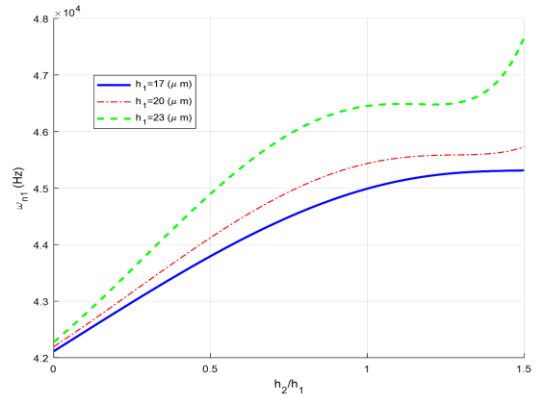

Fig. 2. Variation of the first natural frequency of the microsensor versus the ratio thickness of layers $\frac{h_2}{h_1}$ for different values of the silicon layer thickness h_1

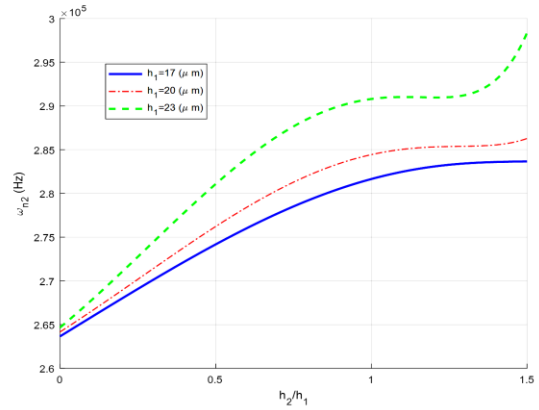

Fig. 3. Variation of the second natural frequency of the microsensor versus the ratio thickness of layers $\frac{h_2}{h_1}$ for different values of the silicon layer thickness h_1

It should be noted that there is interesting behavior on the natural frequencies with the increase of dimensionless thickness parameter h_2/h_1 which can be considered in the optimization design of the sensor. The above behavior for second and third natural frequencies of the microsensor can also be observed in Figures 3 and 4, respectively.

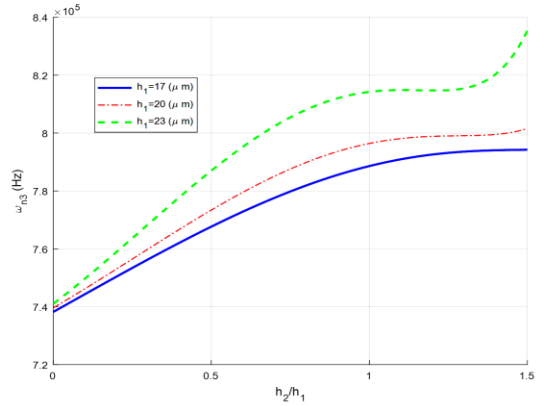

Fig. 4. Variation of the third natural frequency of the microsensor versus the ratio thickness of layers $\frac{h_2}{h_1}$ for different values of the silicon layer thickness h_1

Also, the first natural frequency of the microsensor versus piezoelectric thickness h_2 has been depicted in Figure 5 for various values of dimensionless material length scale parameter l_1/h_1, at silicon thickness $h_1 = 20$ μm. The results in Figure 5 show that the first natural frequency of the microsensor will decrease when dimensionless material length scale parameter l_1/h_1 increases.

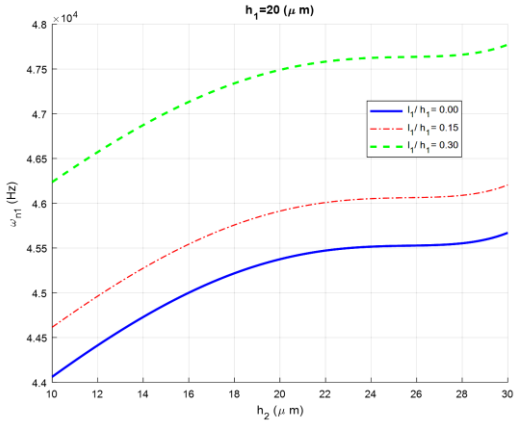

Fig. 5. Variation of the first natural frequency of the microsensor versus thickness of the piezoelectric layer h_2 for different values of dimensionless material length scale parameter l_1/h_1

In addition, the variation of the first natural frequency of the system versus the dimensionless parameter L/w has been investigated in Figure 6 for different values of the silicon thickness h_1 and piezoelectric thickness h_2, at sensor length $L = 800$ μm. The obtained results in Figure 6 show that the first natural frequency of the microsensor will decrease with either increasing dimensionless parameter L/w or decreasing the thickness of silicon and piezoelectric layers. It should be noted that the behavior of the second and third natural frequencies of the system are the same as Figures 5 and 6. Therefore, only the first natural frequency (fundamental natural frequency) of the system are presented.

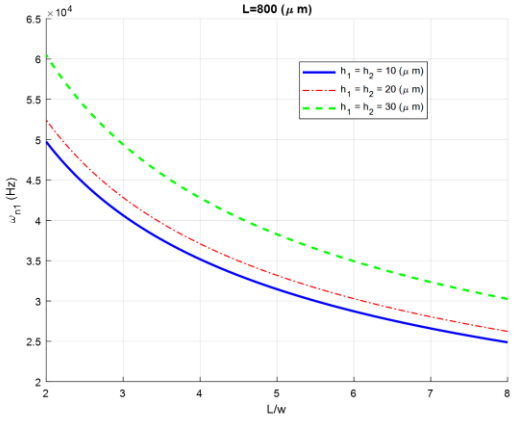

Fig. 6. Variation of the first natural frequency of the microsensor versus the dimensionless parameter $\frac{L}{w}$ for different values of the thickness of the layers h_1 and h_2

SUMMARY AND CONCLUSION

In this paper, the dynamic behavior of a microsensor with two layers of the silicon and piezoelectric was investigated by an analytical approach. To capture size effects and to predict the vibration behavior of the microsensor, governing equations were derived based on the Modified Couple Stress Theory (MCST) and Hamilton's principle. The analytical method was employed in the solution of the partial differential equations. The first, second and third natural frequencies of the system for various values of system parameters such as dimensionless material length scale parameter l_1/h_1, the thickness of the silicon and piezoelectric layers, dimensionless parameters h_2/h_1 and L/w were studied. The presented analytical method can predict the effect of size-dependency on the dynamic behavior of a microsensor with two layers of silicon and piezoelectric, based on the MCST. Moreover, the presented analytical solution can be used for design and optimization of the microsensors.

The obtained results of the natural frequencies of the system with respect to different values of system parameters were presented. The results show that material length scale parameter values, as well as length, width, and thickness of each layer, have significant effects on the vibration response of the microsensor. In addition, the obtained results show an interesting behavior of the natural frequencies with respect to the variation of dimensionless thickness parameter h_2/h_1. This characteristic can be used to optimize the design of microsensors.

REFERENCES

[1] Rezazadeh G, Tahmasebi A, Zubstov M. Application of piezoelectric layers in electrostatic MEM actuators: controlling of pull-in voltage. Microsystem technologies. 2006 Oct 1;12(12):1163-70.

[2] Hu YC, Chang CM, Huang SC. Some design considerations on the electrostatically actuated microstructures. Sensors and Actuators A: Physical. 2004 Apr 15;112(1):155-61.

[3] Mahdavi MH, Farshidianfar A, Tahani M, Mahdavi S, Dalir H. A more comprehensive modeling of atomic force microscope cantilever. Ultramicroscopy. 2008 Dec 1;109(1):54-60.

[4] McMahan LE, Castleman BW. Characterization of vibrating beam sensors during shock and vibration. InPLANS 2004. Position Location and Navigation Symposium (IEEE Cat. No. 04CH37556) 2004 Apr 26 (pp. 102-110). IEEE.

[5] Coutu Jr RA, Kladitis PE, Starman LA, Reid JR. A comparison of micro-switch analytic, finite element, and experimental results. Sensors and Actuators A: Physical. 2004 Sep 21;115(2-3):252-8.

[6] Duc TC, Creemer JF, Sarro PM. Piezoresistive cantilever beam for force sensing in two dimensions. IEEE sensors journal. 2006 Dec 26;7(1):96-104.

[7] Abdel-Rahman EM, Younis MI, Nayfeh AH. Characterization of the mechanical behavior of an electrically actuated microbeam. Journal of Micromechanics and Microengineering. 2002 Sep 5;12(6):759.

[8] Zand MM, Ahmadian MT. Vibrational analysis of electrostatically actuated microstructures considering nonlinear effects. Communications in Nonlinear Science and Numerical Simulation. 2009 Apr 1;14(4):1664-78.

[9] Coutu Jr RA, Kladitis PE, Starman LA, Reid JR. A comparison of micro-switch analytic, finite element, and experimental results. Sensors and Actuators A: Physical. 2004 Sep 21;115(2-3):252-8.

[10] Orhan S. Analysis of free and forced vibration of a cracked cantilever beam. Ndt & E International. 2007 Sep 1;40(6):443-50.

[11] Barad KH, Sharma DS, Vyas V. Crack detection in cantilever beam by frequency based method. Procedia Engineering. 2013 Jan 1;51:770-5.

[12] Lam DC, Yang F, Chong AC, Wang J, Tong P. Experiments and theory in strain gradient elasticity. Journal of the Mechanics and Physics of Solids. 2003 Aug 1;51(8):1477-508.

[13] Fleck NA, Muller GM, Ashby MF, Hutchinson JW. Strain gradient plasticity: theory and experiment. Acta Metallurgica et Materialia. 1994; 42(2): 475-487.

[14] Stölken JS, Evans AG. A microbend test method for measuring the plasticity length scale. Acta Materialia. 1998 Sep 1;46(14):5109-15..

[15] Lam DC, Chong AC. Indentation model and strain gradient plasticity law for glassy polymers. Journal of materials research. 1999; 14(09): 3784-3788.

[16] Chong AC, Lam DC. Strain gradient plasticity effect in indentation hardness of polymers. Journal of Materials Research. 1999; 14(10): 4103-4110.

[17] Eringen AC. Nonlocal polar elastic continua. International journal of engineering science. 1972; 10(1): 1-16.

[18] Mindlin RD, Eshel NN. On first strain-gradient theories in linear elasticity. International Journal of Solids and Structures. 1968; 4(1): 109-124.

[19] Fleck NA, Hutchinson JW. A phenomenological theory for strain gradient effects in plasticity. Journal of the Mechanics and Physics of Solids. 1993; 41(12): 1825-1857.

[20] Lam DC, Yang F, Chon, ACM, Wang J, Tong P. Experiments and theory in strain gradient elasticity. Journal of the Mechanics and Physics of Solids. 2003; 51(8): 1477-1508.

[21] Mindlin RD, Tiersten HF. Effects of couple-stresses in linear elasticity. Archive for Rational Mechanics and analysis. 1962; 11(1): 415-448.

[22] Yang FACM, Chong ACM, Lam DC, Tong P. Couple stress based strain gradient theory for

elasticity. International Journal of Solids and Structures. 2002; 39(10): 2731-2743.
[23] Asghari M, Kahrobaiyan MH, Rahaeifard M, Ahmadian MT. Investigation of the size effects in Timoshenko beams based on the couple stress theory. Archive of Applied Mechanics. 2011; 81(7): 863-874.
[24] Park SK, Gao XL. Bernoulli–Euler beam model based on a modified couple stress theory. Journal of Micromechanics and Microengineering. 2006; 16(11): 2355-2359.
[25] Ma HM, Gao XL, Reddy JN. A microstructure-dependent Timoshenko beam model based on a modified couple stress theory. Journal of the Mechanics and Physics of Solids. 2008; 56(12): 3379-3391.
[26] Ghiasi EK. Application of modified couple stress theory to study dynamic characteristics of electrostatically actuated micro-beams resting upon squeeze-film damping under mechanical shock. International Journal of Advanced Mechanical Engineering. 2016; ISSN 2250-3234 6(1): 1-15.
[27] Liang LN, Ke LL, Wang YS, Yang J, Kitipornchai S. Flexural vibration of an atomic force microscope cantilever based on modified couple stress theory. International Journal of Structural Stability and Dynamics. 2015; 15(07): 1540025.
[28] Dai HL, Wang YK, Wang L. Nonlinear dynamics of cantilevered microbeams based on modified couple stress theory. International Journal of Engineering Science. 2015; 94: 103-112.
[29] Ke LL, Wang YS. Size effect on dynamic stability of functionally graded microbeams based on a modified couple stress theory. Composite Structures. 2011; 93(2): 342-350.
[30] Li X, Luo Y. Flexoelectric effect on vibration of piezoelectric microbeams based on a modified couple stress theory. Shock and Vibration, 2017.
[31] Ghayesh MH, Farokhi H. Nonlinear dynamics of microplates. International Journal of Engineering Science. 2015; 86: 60-73.
[32] Simsek M, Aydın M. Size-dependent forced vibration of an imperfect functionally graded (FG) microplate with porosities subjected to a moving load using the modified couple stress theory. Composite Structures. 2017; 160: 408-421.
[33] Guo J, Chen J, Pan E. Free vibration of three-dimensional anisotropic layered composite nanoplates based on modified couple-stress theory. Physica E: Low-dimensional Systems and Nanostructures. 2017; 87: 98-106.
[34] Askari AR, Tahani M. Size-dependent dynamic pull-in analysis of geometric non-linear micro-plates based on the modified couple stress theory. Physica E: Low-dimensional Systems and Nanostructures. 2017; 86: 262-274.
[35] Akbas SD. Free vibration of edge cracked functionally graded microscale beams based on the modified couple stress theory. International Journal of Structural Stability and Dynamics. 2017; 17(03): 1750033.
[36] Alinaghizadeh F, Shariati M, Fish J. Bending analysis of size-dependent functionally graded annular sector microplates based on the modified couple stress theory. Applied Mathematical Modelling. 2017.
[37] He D, Yang W, Chen W. A size-dependent composite laminated skew plate model based on a new modified couple stress theory. Acta Mechanica Solida Sinica. 2017; 30(1), 75-86.
[38] Shafiei N, Mousavi A, Ghadiri M. Vibration behavior of a rotating non-uniform FG microbeam based on the modified couple stress theory and GDQEM. Composite Structures. 2016; 149: 157-169.
[39] Li X, Luo Y. Flexoelectric effect on vibration of piezoelectric microbeams based on a modified couple stress theory. Shock and Vibration. 2017;2017.
[40] Shoaib M, Hisham N, Basheer N, Tariq M. Frequency and displacement analysis of electrostatic cantilever-based MEMS sensor. Analog Integrated Circuits and Signal Processing. 2016 Jul 1;88(1):1-1.
[41] Shoaib M, Hisham N, Basheer N, Tariq M. Frequency analysis of electrostatic cantilever-based MEMS sensor. In2015 Symposium on Design, Test, Integration and Packaging of MEMS/MOEMS (DTIP) 2015 Apr 27 (pp. 1-6). IEEE.
[42] Shoaib M, Hamid NH, Jan MT, Ali NB. Effects of crack faults on the dynamics of piezoelectric cantilever-based MEMS sensor. IEEE Sensors Journal. 2017 Aug 7;17(19):6279-94.